Physiological and Molecular Plant Pathology 114 (2021) 101630

Contents lists available at ScienceDirect

Physiological and Molecular Plant Pathology

journal homepage: www.elsevier.com/locate/pmpp

The Mi-EFF1/Minc17998 effector interacts with the soybean GmHub6 protein to promote host plant parasitism by *Meloidogyne incognita*

Reneida Aparecida Godinho Mendes [a,b,1], Marcos Fernando Basso [a,i,1], Bruno Paes de Melo [a,c], Thuanne Pires Ribeiro [a,b], Rayane Nunes Lima [a], Janaina Fernandes de Araújo [a], Maira Grossi-de-Sa [d], Vanessa da Silva Mattos [a], Roberto Coiti Togawa [a], Érika Valéria Saliba Albuquerque [a], Maria Eugênia Lisei-de-Sa [a,e], Maria Cristina Mattar da Silva [a], Leonardo Lima Pepino Macedo [a], Rodrigo da Rocha Fragoso [f], Diana Fernandez [a,d], Florence Vignols [g], Maria Fatima Grossi-de-Sa [a,h,i,*]

[a] *Embrapa Genetic Resources and Biotechnology, Brasília-DF, 70297-400, Brazil*
[b] *Federal University of Brasília, Brasília-DF, 70910-900, Brazil*
[c] *Federal University of Viçosa, Viçosa-MG, 36570-900, Brazil*
[d] *IRD, Cirad, Univ Montpellier, IPME, 911, Avenue Agropolis, 34394, Montpellier Cedex 5, France*
[e] *Agricultural Research Company of Minas Gerais, Uberaba-MG, 38060-040, Brazil*
[f] *Embrapa Cerrados, Planaltina-DF, 73310-970, Brazil*
[g] *Biochimie et Physiologie Moléculaire des Plantes, CNRS/INRA/Université de Montpellier/SupAgro, Montpellier, France*
[h] *Catholic University of Brasília, Brasília-DF, 71966-700, Brazil*
[i] *National Institute of Science and Technology-INCT PlantStress Biotech-EMBRAPA, Brazil*

ARTICLE INFO

Keywords:
Root-knot nematodes
Effector secretion
Protein-protein interaction
Nematode control

ABSTRACT

Meloidogyne incognita is the most frequently reported specie in the root-knot nematode (RKN) responsible for damage to several different crops worldwide. The interaction between *M. incognita* and host plants involves the secretions of molecular factors from the nematode, which mainly suppress the defense response and promote plant parasitism. On the other hand, several plant elements are associated with the immune defense system that opposes nematode infection. In this study, the interaction of the Mi-EFF1/Minc17998 effector with the soybean GmHub6 (Glyma.17G099100; TCP14) protein was identified and characterized *in vivo* and *in planta*. Data showed that the *GmHub6* gene is upregulated by *M. incognita* infection in a nematode-resistant soybean genotype (PI595099) compared to a susceptible cultivar (BRS133). As a result, the *Arabidopsis thaliana AtHub6* mutant ($AtHub6^{KO}$) line (AT3G47620, an orthologous gene of *GmHub6*) exhibited normal vegetative development of the plant but was more susceptible to *M. incognita*. Thus, since the soybean and *A. thaliana* Hub6 proteins are TEOSINTE BRANCHED/CYCLOIDEA/PCF (TCP) transcription factors involved in plant development and morphogenesis modulation, flowering time regulation, and activation of the plant immune system, our data suggest that the interaction of Mi-EFF1/Minc17998 and Hub6 proteins is associated with an increase in plant susceptibility to nematode infection during parasitism. It is suggested that this interaction may prevent the nuclear localization or disturb the activity of GmHub6 as a typical transcription factor modulating the cell cycle of the plant, avoid the activation of the host's defense response, and successfully promote parasitism. Our findings indicate the potential of the Mi-EFF1/Minc17998 effector for the development of biotechnological tools based on the RNA interference approaches and *GmHub6* gene overexpression for the RKN control.

* Corresponding author. Embrapa Genetic Resources and Biotechnology, PqEB Final, W5 Norte, PO Box 02372, 70770-901, Brasília-DF, Brazil.
E-mail address: fatima.grossi@embrapa.br (M.F. Grossi-de-Sa).
[1] Both authors contributed equally.

https://doi.org/10.1016/j.pmpp.2021.101630
Received 24 November 2020; Received in revised form 1 February 2021; Accepted 8 February 2021
Available online 17 February 2021

1. Introduction

Meloidogyne incognita is a biotrophic pathogen and obligate sedentary endoparasite belonging to the root-knot nematode (RKN), which consists of the unique genus *Meloidogyne* spp. [1,2]. The RKN life cycle consists of six stages: egg, J1 (first-stage juvenile), J2 (second-stage juvenile), J3 (third-stage juvenile), J4 (fourth-stage juvenile), and adult (female and male). The J3, J4, and female individuals are typically sedentary endophytes, while the egg, J1, and preparasitic J2 stages are exophytes in most *Meloidogyne* species [2–4]. The *M. incognita* is one of the major agricultural pathogens responsible for significant annual economic losses worldwide [5]. It disturbs plant roots by altering the cell cycle, increasing parasitized cells' size, causing cell hyperproliferation and the development of giant cells [6–10]. These disorders disrupt water and nutrient uptake by the roots and may reduce plant growth and yield [11–13].

The interaction between *M. incognita* and host plants involves an extensive molecular immunity network involved in defense and counter-defense [14,15]. In addition to basal defense mechanisms, after the recognition of nematode elicitors, host plants increase the production of reactive oxygen and nitrogen species and other toxic compounds derived from secondary metabolism [16–19]. In contrast, *M. incognita* increases the production and release of antioxidant and detoxifying compounds [20–23] and, particularly, effector proteins to overcome host defense [24–26]. Thus, several nematode effector proteins modulate different biological processes and defense responses of the host plant [24,26–30]. For example, *Mi*-MSP18 [28] and *Mi*-Msp40 [31] effectors function in cell death suppression and can increase plant susceptibility and modulate host immunity. Likewise, the Mi8D05 effector interacts with the plant tonoplast intrinsic protein 2 (TIP2) aquaporin, suggesting that it regulates solute and water transport within giant cells [32]. Other examples include MiPFN3, which disrupts the plant's actin cytoskeleton [33], while MiMIFs interfere with annexin-mediated plant immune responses [30] to promote plant infection.

In this context, secretome analyses of *M. incognita* J2 preparasites allowed the identification of numerous candidate effector proteins [20,34–36], but their roles in host parasitism are still not well understood. By applying comparative genomic approaches to EST datasets, Jaouannet et al. [37] identified at least three genes that were specifically expressed in the esophageal glands of parasitic *M. incognita* juveniles. Among these genes, the Mi-EFF1/Minc17998 effector is secreted during parasitism within giant cells and targets the nuclei. Therefore, the Mi-EFF1/Minc17998 effector has been suggested to be involved in the manipulation of the host cell nuclear functions [37]. Nevertheless, the precise role of this effector during plant parasitism has not yet been demonstrated. Previous studies on protein-protein interactions between *Arabidopsis thaliana* and different phytopathogens (bacteria, oomycetes, and fungi) showed that several pathogen effector proteins preferentially interact with a limited set of highly connected (hub) proteins of the host plant [38–40]. The AtHub6 (AT3G47620), the most targeted hub protein, was shown to interact with four effectors from the bacterium *Pseudomonas syringae,* 25 effectors from the oomycete *Hyaloperonospora arabidopsidis* [38], and 23 effectors from the fungus *Golovinomyces orontii* [39]. Interestingly, AtHub6 is a TEOSINTE BRANCHED/CYCLOIDEA/PCF (TCP) 14 (AtTCP14) transcription factor that transcriptionally activates or interacts with numerous other plant proteins associated with cell cycle control, plant development [41–46], and to the regulation of the immune system [38,42,47–49]. Curiously, Yang et al. [48] showed that the *P. syringae* HopBB1 effector interacts with the AtTCP14 protein and targets it to the SCF^{COI1} degradation complex, thus promoting bacterial virulence. Similarly, the *A. thaliana* triple T-DNA insertion mutant for the *AtTCP8*, *AtTCP14*, and *AtTCP15* genes (*tcp8*, *tcp14*, and *tcp15*) proved to be more susceptible to *P. syringae* pv. *maculicola* than wild-type (WT) plants [47]. Additionally, Spears et al. [43] demonstrated that the *A. thaliana tcp8 tcp14 tcp15* triple mutant exhibited impairment of pathogen-associated molecular pattern (PAMP)-triggered immunity (PTI), which is one layer of the plant innate immune system. Despite its involvement in the plant developmental and defense responses, there is no information on the interaction of AtHub6 with nematode effectors and the role of these protein-protein interactions in plant susceptibility to nematode infection.

Soybean (*Glycine max*) is one of the most important agricultural commodities worldwide and is indispensable for human and animal nutrition [50,51]. However, soybean crop expansion and yields have been limited by nematode incidence [52]. The main commercial soybean cultivars are susceptible to nematode infections and, under inefficient nematode management, significant yield and economic losses are caused annually by RKNs, including *M. incognita* [53]. Thus, a better understanding of the molecular interactions between soybean and nematodes could allow the development of new biotechnological tools (NBTs) for RKN control [54,55]. Herein, we identified and validated the interaction between the Mi-EFF1/Minc17998 effector and the soybean GmHub6 protein (ortholog of AtHub6) using *in vivo* and *in planta* approaches. Curiously, our data obtained by using an *A. thaliana* T-DNA mutant of the *AtHub6* gene suggested that the disruption of AtHub6 protein function can be associated with an increase in plant susceptibility to nematode infection. Therefore, our data strongly indicate that this interaction can modulate the development of parasitized cells, prevent the activation of the immune system and, consequently, support the parasitism of the host plant.

2. Materials and methods

2.1. In silico analyses of the M. incognita Mi-EFF1/Minc17998 effector and soybean GmHub proteins

All sequences of *M. incognita* effector genes were retrieved from BioProject ID PRJEB8714 (sample ERS1696677) [56] from the online WormBase Parasite Database version WBPS13 [57]. Pairwise identity matrices for nucleotide and amino acid sequences were generated using Sequence Demarcation Tool Version 1.2 software [58]. Phylogenetic analyses of the *M. incognita* effector sequences were performed using the Phylogeny.fr web service [59]. For these analyses, sequences were aligned with MUSCLE software [60], and the alignment was curated by the Gblocks model. Then, phylogenetic analyses were performed using the maximum likelihood method with PhyML software using an approximate likelihood-ratio test (aLRT) SH-like branch support and the GTR and WAG substitution models for nucleotide and amino acid sequences, respectively. Phylogenetic trees were generated and visualized with TreeDyn software, which was implemented at the same web service. Comparative genomic trees were generated from BioProject PRJEB8714 [56] by the WormBase ParaSite Database using the Ensembl Compara tools. The *in silico* expression levels of Mi-EFF1/Minc17998 and of its paralogous *Minc3s01563g24741* gene at different *M. incognita* life stages were determined using transcriptome datasets (BioProject number: PRJNA390559; [61]) retrieved from the BioSample database (NCBI). For this analysis, 15 transcriptome libraries from the *M. incognita* egg, J2, J3, J4, and female stages generated by Choi et al. [61] using the Truseq RNA Sample Prep Kit (Illumina) and mRNAs that were paired-end sequenced (2 x 101 bp) using Illumina HiSeq 2000 technology were downloaded and trimmed, and the transcripts were mapped using the genome reference retrieved from the WormBase Parasite Database (BioProject ID PRJEB8714) [62]. The gene expression profiles in different nematode life stages were normalized to transcripts per million (TPM) values.

On the other hand, the sequences and characteristics of soybean genes were retrieved from *G. max Wm82.a2.v1* (BioProject: PRJNA19861) [63] via the Phytozome v.12 database [64]. Conserved domains in the gene sequences were identified using the NCBI CDD Database [65], the annotation was confirmed by the HMMER prediction server [66], and the nuclear signal localization (NLS) motifs were predicted using the NLStradamus online tool [67]. The pairwise identity

matrices were generated, and phylogenetic analyses were performed as described above. The interactome network of soybean and *A. thaliana* hub proteins with their interacting proteins was retrieved from the STRING database v.11 platform [68]. The organ- and tissue-specific expression of the eight *GmHub* genes, including the top 10 soybean proteins with which GmHub6 interacted, is presented in the heat map plot generated by the PhytoMine tool (https://phytozome.jgi.doe.gov/phytomine/begin.do) using all gene expression data in the database related to tissue- and organ-specific expression.

2.2. Mi-EFF1/Minc17998 expression profile determined using RT-qPCR assays

The *Mi-EFF1/Minc17998* gene expression levels in different nematode life stages (egg, J2, J2/J3, J3/J4, and female) during plant infection were determined using tomato roots inoculated with 500 *M. incognita* J2 race 3 individuals. Total RNA was isolated using the Concert™ Plant RNA Reagent (Invitrogen, Carlsbad, CA, USA) supplemented with PVP-40. The RNA concentration was estimated using a spectrophotometer (NanoDrop 2000, Thermo Scientific, Massachusetts, USA), and RNA integrity was evaluated via 1% agarose gel electrophoresis. The RNA samples were treated with RNase-free RQ1 DNase I (Promega, Madson, Wisconsin, USA) according to the manufacturer's instructions. Then, 2–4 μg of DNase-treated RNA was employed in the cDNA synthesis using oligo-$(dT)_{20}$ primers and SuperScript III RT (Life Technologies, Carlsbad, CA, USA), according to the manufacturer's instructions. The cDNA was quantified by spectrophotometry and diluted 1/10 with nuclease-free water. RT-qPCR assays were performed in an Applied Biosystems 7500 Fast Real-Time PCR System (Applied Biosystems, Foster City, CA, USA) using 400 ng of cDNA, each primer gene-specific at 0.2 μM (Table S1) and GoTaq® qPCR Master Mix (Promega, Madson, Wisconsin, USA). The qPCR conditions included an initial step at 95 °C for 10 min, then 40 cycles of 95 °C for 15 s and 60 °C for 1 min, followed by a final melting curve analysis. The relative expression of the *Mi-EFF1/Minc17998* gene was normalized using *Mi18S* (GenBank accession U81578) [69] as an endogenous reference gene. Three biological replicates composed of one plant each were performed, and the cDNA samples were used in technical triplicate reactions. Primer efficiency and target-specific amplification were confirmed based on a single distinct peak in the melting curve analysis. The relative expression level was calculated using the $2^{-\Delta Ct}$ method [70].

2.3. In vivo and in planta transactivation assays for the evaluation of protein-protein interactions

Protein-protein interaction tests were performed to evaluate the interaction of the Mi-EFF1/Minc17998 effector with eight soybean hub proteins: GmHub4 (COP9 signalosome complex subunit 5), GmHub6 (TCP family transcription factor), GmHub10 (kinesin light chain), GmHub12 (APC8/anaphase-promoting complex subunit), GmHub17 (TCP family transcription factor), GmHub42 (transcription factor UNE12-related), GmHub47 (jasmonate ZIM domain-containing protein), and GmHub61 (uncharacterized conserved protein containing an emsy amine-terminus domain) (Table 1). The cDNA sequences of the soybean hub proteins were amplified from total RNA isolated from the roots of the soybean cv. Williams 82. Amplicons of the expected size were cloned into the pGEM-T Easy vector (Promega, Madson, Wisconsin, USA) and sequenced by Macrogen (Geumcheon-gu, Seoul, South Korea); after sequence analyses, desirable amplicons were subcloned based on the restriction sites present in the primers into the entry vector of the Gateway cloning system (pENTR11; Invitrogen, Carlsbad, CA, USA). Sequence identities were confirmed by comparison with gene sequences retrieved from *G. max Wm82.a2.v1* (BioProject: PRJNA19861) [63] via the Phytozome v.12 database [64]. The transfer of the cDNA clones from the entry vector to the pGADT7-AD, pGBKT7-BD, and BiFC destination vectors was performed using the Gateway ™ LR Clonase ™ II system (Invitrogen, Carlsbad, CA, USA). The full-length cDNA sequence of the Mi-EFF1/Minc17998 effector was synthesized by Epoch Life Science (Sugar Land, TX, USA), cloned into the pENTR11 vector, propagated in *E. coli* DH5α, and subsequently transferred to the pGADT7-AD and pGBKT7-BD destination vectors using the LR clonase system. Y2H experiments were performed using the Matchmaker™ GAL4 Two-Hybrid System 3 (Clontech, Mountain View, CA, USA) based on the GAL4 binding (BD) and transactivation (AD) domains present in these destination vectors. Both Y2H vectors were sequentially cotransformed into competent cells of the *Saccharomyces cerevisiae* YRG2 strain (Matα, ura3-52, his3-200, ade2-101, lys2-801, trp1-901, leu2-3, 112, gal4-542, gal80-538) using the lithium acetate/polyethylene glycol (PEG) method. Single colonies of cotransformed yeast were grown overnight in selective yeast nitrogen base (YNB) medium in a shaking incubator at 180 rpm at 30 °C. Yeast cells were diluted in fresh YNB medium to an optical dilution (OD_{600}) of approximately 1 to 0.01. Then, 100 μl of the suspension was plated on synthetic dropout medium lacking leucine, tryptophan, and histidine and containing the 3-amino-1,2,4-triazole

Table 1
Features of the eight soybean GmHub proteins retrieved from the *G. max* Wm82.a2.v1 (BioProject: PRJNA19861) genome dataset from the Phytozome v.12 database.

Soybean GmHubs	Gene ID	Gene function annotations	TAIR	Gene/ CDS length	Chr	Chromosome location (START/ END)	Protein aa/kDa	CDD domain search	HMMER prediction	NLS motif
GmHub4	Glyma.06G076000	COP9 signalosome complex subunit 5, CSN5	AT1G22920	4154/ 1230	06	5880948/ 5885101	409/ 45.9	cd08069	PF01398.21 PF18323.1	no
GmHub6	Glyma.17G099100	TCP family transcription factor	AT3G47620	3003/ 1242	17	7811940/ 7814942	413/ 44.8	pfam03634	PF03634.13	yes
GmHub10	Glyma.19G008200	Kinesin light chain	AT3G27960	3623/ 2103	19	810694/814316	700/ 77.07	pfam13424	PF13424.6 PF13176.6	yes
GmHub12	Glyma.11G026400	APC8/Anaphase promoting complex subunit	AT3G48150	3708/ 1734	11	1877873/ 1881580	577/ 67.1	pfam04049 cl37187	PF04049.13 PF13181.6 PF13414.6 PF13176.6	no
GmHub17	Glyma.02G105900	TCP family transcription factor	AT1G69690	2169/ 1275	02	10090282/ 10092450	424/ 44.1	pfam03634	PF03634.13	yes
GmHub42	Glyma.19G160900	Transcription factor UNE12-Related	AT4G02590	4204/ 879	19	42160254/ 42164457	292/ 31.2	cd18919	PF00010.26	yes
GmHub47	Glyma.09G174200	Jasmonate ZIM domain-containing protein	AT3G17860	6521/ 1161	09	39883774/ 39890294	386/ 41.5	pfam06200 pfam09425	PF06200.14 PF09425.10	no
GmHub61	Glyma.02G178800	Uncharacterized conserved protein containing an emsy amine-terminus domain	AT5G06780	7710/ 1275	02	30282810/ 30290519	424/ 47.4	pfam03735 smart00743	PF03735.14	no

Chr: chromosome; aa: amino acid.

(3-AT) *His3* gene-product competitive inhibitor at 5–10 mM, followed by incubation at 28 °C for three to five days. The empty pGADT7-AD and pGBKT7-BD vectors were used as negative controls for protein-protein interactions, while pGADT7-AD:NIG and pGBKT7-BD:AtWWP1 were used as positive controls. The *A. thaliana* AtWWP1 (AT2G41020) and NIG (AT4G13350) protein interactions were previously validated by Calil et al. [71].

BiFC assays were carried out using different combinations of the *A. tumefaciens* GV3101 strain carrying pSITE BiFC cEFYP (GU734652) and nEYFP (GU734651) binary vectors containing the 35S:GmHub6-cYFP and 35S:Mi-EFF1/Minc17998-nYFP fusion proteins. An *A. tumefaciens* coculture was coinfiltrated into the abaxial surface of *N. tabacum* leaves at an OD_{600} nm of 0.7 at a final ratio of 1:1. Yellow fluorescence was analyzed in epidermal cells three days after infiltration using a Zeiss inverted LSM510 META laser scanning microscope equipped with an argon laser and a helium laser as excitation sources. Yellow fluorescent protein (YFP) was excited at 514 nm using an argon laser, and YFP emission was detected using a 560-615-nm filter.

2.4. GmHub6 expression profile in soybean roots during M. incognita infection

M. incognita J2 race 1 was obtained from tomato plants (*Solanum lycopersicum* cv. Santa Clara) that were inoculated and maintained for eight to ten weeks under greenhouse conditions. Infected roots were washed and macerated using a blender after treatment with 0.5% sodium hypochlorite. Eggs were harvested, rinsed with tap water, and subsequently separated from root debris using 100- to 550-μm sieves [72]. Then, the eggs were hatched under aerobic conditions at 28 °C, and J2 individuals were harvested every two days, decanted and quantified under a microscope using a counting chamber. The conventional soybean genotype PI595099 (resistant) and cultivar BRS133 (susceptible), which are considered exhibiting contrasting RKN resistance levels [73], were inoculated with 1,000 newly hatched *M. incognita* J2 individuals, and axillary root samples were harvested at 3 (plant developmental stage I), 8 (plant developmental stage II), 15 (plant developmental stage III), and 25 dpi (plant developmental stage IV) from mock- and nematode-inoculated plants. Total RNA was purified using the Concert™ Plant RNA Reagent (Invitrogen, Carlsbad, CA, USA) supplemented with PVP-40, and cDNA was synthesized from DNA-free, highly pure RNA as described above. The expression profile of the *GmHub6* gene during nematode infection was measured by RT-qPCR assays using specific primers and normalized with *GmCYP18* (Glyma.12G024700) as an endogenous reference gene (Table S1). The thermocycling reactions and conditions used were the same as those described above. Four biological replicates were performed for each treatment, and each biological replicate was composed of four plants. All cDNA samples were used in technical triplicates, and primer efficiency and target-specific amplification were confirmed by a single, distinct peak in the melting curve analysis. The relative expression level was calculated using the $2^{-\Delta Ct}$ method [70].

2.5. M. incognita resistance assessment of the AtHub6^{KO}

The *A. thaliana* seeds from the *AtHub6* gene mutant line *hub6* (T-DNA insertion; *attcp14-5*, GK-611C04/CS458588, of AT3G47620, an orthologous gene of soybean *GmHub6*; Additional file 1) and the null mutant line for the *enhanced disease susceptibility 1* (*eds1*; AT3G48090; SALK_034340) gene were obtained from the Arabidopsis Biological Resource Center (ABRC; Columbus OH, 43210, USA). The *A. thaliana* seeds were surfaced sterilized and sown in Murashige and Skoog (MS)-containing agar plates. The plates were stratified in the dark at 4 °C for 72 h. Plants were grown in a growth chamber at 22 °C under a 12 h light/12 h dark photoperiod. For growth under *in vivo* conditions, plants from the WT, *AtEds1*, and *AtHub6* lines were transferred to 1:1 substrate: sand (autoclaved commercial substrate and sand at a 1:1 ratio) and grown as described above. Then, three-week-old plants were inoculated with 250 J2 individuals of *M. incognita* race 3 as described above. The inoculated roots were harvested at 5, 10, 15, and 25 days post-inoculation (dpi) and stained with acid fuchsin as described by Bybd et al. [74], and the penetration efficiency in the roots, the post penetration development of the nematodes, and the formation of galls were evaluated. In addition, the number of eggs per gram of roots, the number of J2 individuals per gram of roots, the number of galls per plant, and NRF were determined from an additional plant set at 40 dpi. The NRF was determined as described above, and the *AtEds1* mutant line was used as a susceptibility control. *A. thaliana* lines were evaluated in three biological replicates composed of 15–20 plants each replicate.

3. Results

3.1. In silico analysis of the Mi-EFF1/Minc17998 effector sequence

Pairwise comparisons of nucleotide and amino acid sequences showed that the *Mi-EFF1/Minc17998* effector shares a low percentage of nucleotide and amino acid sequence identities with other effectors that are currently better characterized, ranging from 50 to 75% (Fig. 1A) and 15 to 35% (Fig. 1B), respectively. These sequence data suggest that the Mi-EFF1/Minc17998 effector may assume a different functional role from that of the effectors already known in the parasitism of host plants. Two paralogous genes for the Mi-EFF1/Minc17998 effector were identified in the *M. incognita* genome (BioProject PRJEB8714, [56]), which showed considerable homology with its corresponding Mi-EFF1/Minc17998 gene (Supplementary Fig. S1), 99% and 100% (*Minc3s01563g24741* paralog gene) and 92% (*Minc3s06678g40162* paralog gene) sequence identity of the nucleotide and amino acid, respectively. In addition, it has been observed that the Mi-EFF1/Minc17998 effector exhibits relatively conserved orthologous genes in other species of the *Meloidogyne* genus (Supplementary Fig. S1), but their role as effector proteins has not been confirmed yet. Phylogenetic analysis based on nucleotide sequences showed that the Mi-EFF1/Minc17998 effector was clustered with the MiPFN3 and Mj-NULG1a effectors (Fig. 1C), while amino acid sequence analysis showed that the effector was most closely clustered with the Minc00469 and MiISE5 effectors (Fig. 1D). These data obtained from sequence comparisons and the analysis of phylogenetic relationships suggest that the *Mi-EFF1/Minc17998* effector gene does not exhibit a well-defined origin or conserved relationships with other nematode effectors. Transcriptome data mining revealed the expression profiles of the *Mi-EFF1/Minc17998* effector and the *Minc3s01563g24741* gene paralog in different nematode life stages. The two genes showed similar expression levels, with higher expression in the J3, J4, and female stages, while expression was lower in the egg and preparasitic J2 stages (Fig. 1E). RT-qPCR assays revealing the Mi-EFF1/Minc17998 effector expression profile confirmed that expression was higher in the J2/J3, J3/J4, and female stages, but significant expression was also observed in the egg and J2 stages (Fig. 1F). These data showed that *Mi-EFF1/-Minc17998* gene expression is closely associated with the infection stages in the host plant.

3.2. The Mi-EFF1/Minc17998 effector interacts with the soybean GmHub6 protein

In this study, eight of the *A. thaliana* hub proteins previously identified by Mukhtar et al. [38] were selected, and their orthologous soybean genes were identified: GmHub4 (COP9 signalosome complex subunit 5), GmHub6 (TCP family transcription factor), GmHub10 (kinesin light chain), GmHub12 (APC8/anaphase-promoting complex subunit), GmHub17 (TCP family transcription factor), GmHub42 (transcription factor UNE12-related), GmHub47 (jasmonate ZIM domain-containing protein), and GmHub61 (an uncharacterized conserved protein containing an emsy amine-terminus domain)

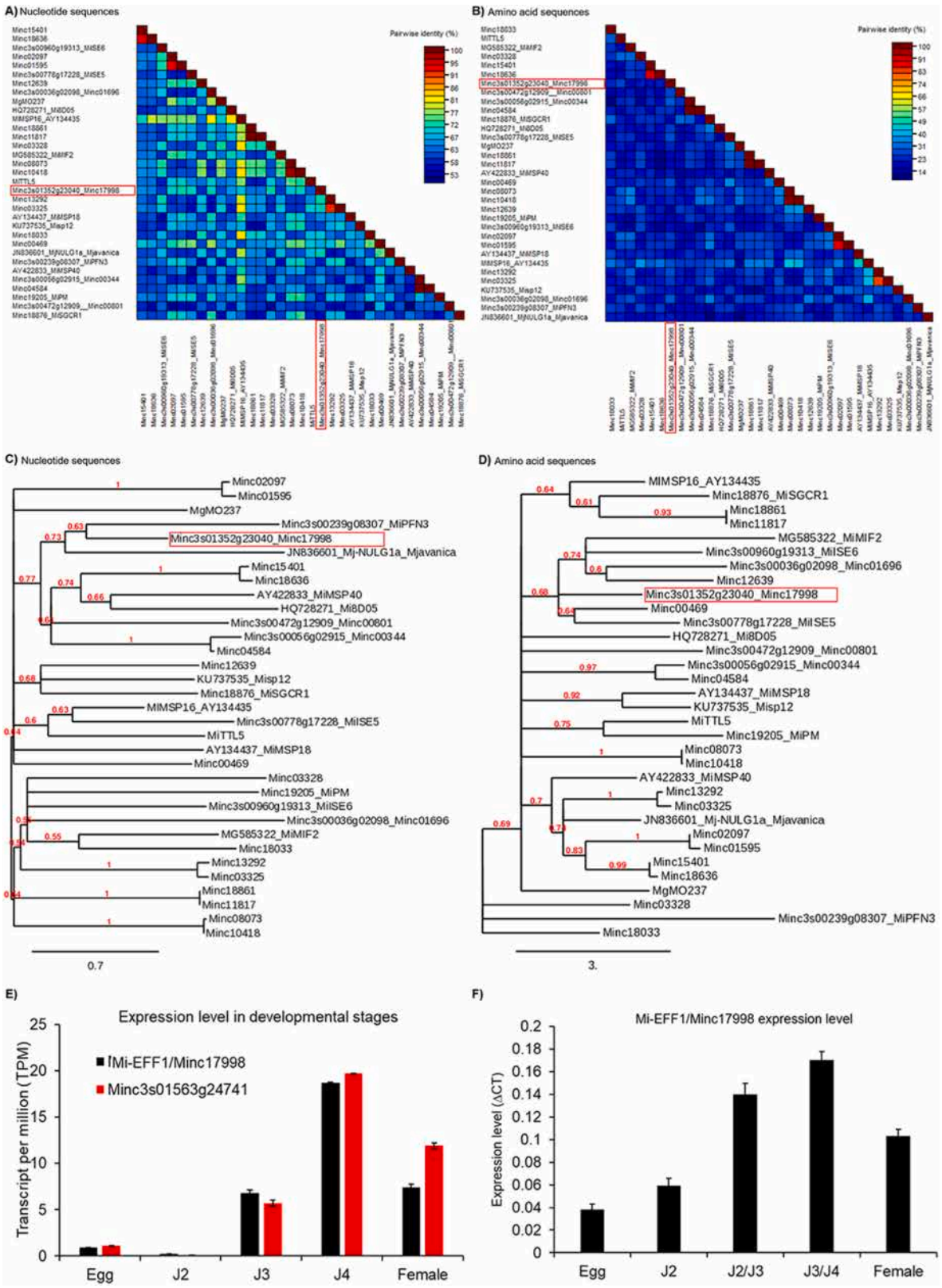

Fig. 1. Sequence analysis and expression profile of the Mi-EFF1/Minc17998 effector. Pairwise sequence identity matrices of **(A)** nucleotide and **(B)** amino acid sequences generated using Sequence Demarcation Tool version 1.2 software. Evolutionary analysis of **(C)** nucleotide and **(D)** amino acid sequences generated by the Phylogeny.fr web service. Gene sequences were retrieved from the online WormBase Parasite Database version WBPS13. **(E)** Expression profile of the nematode *Mi-EFF1/Minc17998* and its paralogous *Minc3s01563g24741* gene in different life stages (egg, J2, J3, J4, and female) of *M. incognita* determined using transcriptome datasets (BioProject number: PRJNA390559) retrieved from the BioSample database (NCBI). Error bars represent confidence intervals corresponding to three libraries per life stage of the nematode. **(F)** Expression profile measured by real-time RT-qPCR of the *Mi-EFF1/Minc17998* effector gene in different life stages of *M. incognita* race 3 during tomato parasitism. The expression level values were calculated by the $2^{-\Delta CT}$ method using the *Mi18S* gene as the endogenous reference gene (Supplementary Table S1). Error bars represent the confidence intervals corresponding to three biological replicates.

(Table 1). Soybean CDS sequences were cloned into the entry and destination vectors to assess the interaction with the Mi-EFF1/Minc17998 effector *in vivo* and *in planta* protein-protein interaction assays. Yeast two-hybrid (Y2H) assays were performed with the soybean proteins and Mi-EFF1/Minc17998, and specific protein-protein interactions were observed only with the GmHub6 protein (Fig. 2A). The Mi-EFF1/Minc17998 effector showed specific interaction with the GmHub6 protein in both Y2H (Fig. 2B and C) and *in planta* by bimolecular fluorescence complementation (BiFC) assays in tobacco (*Nicotiana tabacum*) (Fig. 2D). In addition, both Mi-EFF1/Minc17998 and the GmHub6 protein showed a dimerization ability, but not autoactivation (Fig. 2B). The Mi-EFF1/Minc17998 and GmHub6 interaction was considered relatively strong based on the results of the addition of the 3AT competitive inhibitor to selective medium (Fig. 2C).

3.3. *In silico characterization of the soybean GmHub proteins*

All eight GmHub proteins studied here showed transcript accumulation in almost all plant tissues tested (Supplementary Fig. S2A to S2B). In addition, their protein-protein interaction networks were distinct, except for GmHub10 and GmHub12, which simultaneously interacted with Glyma.07G190600 (anaphase-promoting complex 4) (Supplementary Fig. S2C). The *GmHub6* and its homologous gene (Glyma.05G027400) showed higher amino acid identity with AtHub6 (approx. 55%) and SlTCP14 (approx. 70%), while lower sequence identity (approx. 25%) was observed with other soybean GmHub proteins except for GmHub17 (Fig. 3A). In addition, phylogenetic analysis using amino acid sequences showed that GmHub6 and its homologous gene were grouped close to the TCP transcription factors AtHub6, GmHub17, and SlTCP14 (Fig. 3B). The biological functions of the GmHub6 protein are involved in plant development and the regulation of the defense response, and the protein contains a typical TCP domain (pfam03634) and nuclear localization signal (Tables 1 and 2; Additional file 1). The protein-protein interaction network retrieved from the STRING database highlighted that GmHub6 is the core protein that interacts with numerous other proteins (Supplementary Fig. S3A) similar to the AtHub6 network (Supplementary Fig. S3B). These proteins from the GmHub6 network include several other TCP proteins (Table 2), but considering the orthology with AtHub6, this network of interactions maybe even larger, including dozens of proteins with highly distinct functions [38]. Curiously, *GmHub6* transcripts accumulated in almost all soybean tissues and all different conditions examined, with very low accumulation being observed in the nodules under symbiotic conditions, roots under ammonia treatment, youngest roots, and seeds, in contrast to the relatively high abundance observed in leaves (Supplementary Fig. S3C). In addition, the *GmHub6* gene showed a positive correlation at the expression level with the *Glyma.01G014900*, *Glyma.16G004300*, and *Glyma.18G296100* genes from its network in the same soybean tissues or conditions (Supplementary Fig. S3D).

3.4. *GmHub6 expression profile in soybean roots during M. incognita infection*

RT-qPCR assays showed that the *GmHub6* gene was upregulated in the axillary roots during nematode infection (at 3 dpi) only in the nematode-resistant soybean genotype PI595099 (Fig. 3C). However, the *GmHub6* expression level was similar in the noninoculated roots of both

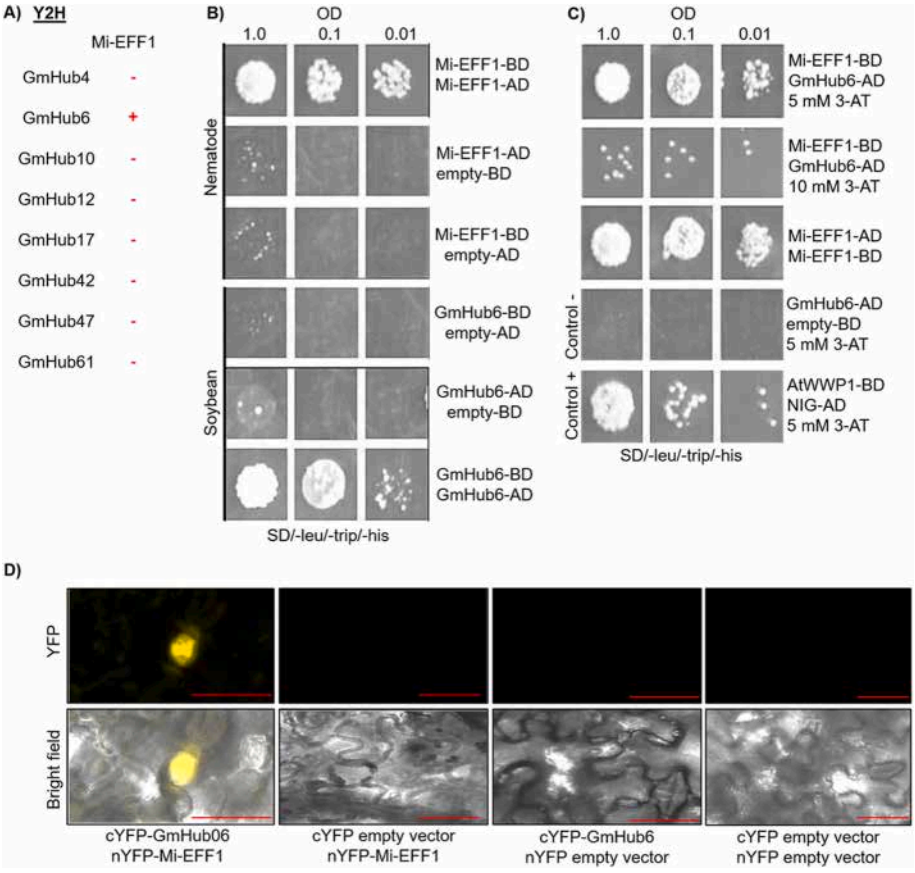

Fig. 2. Protein-protein interaction assays between the Mi-EFF1/Minc17998 effector and eight soybean GmHub proteins. **(A)** Yeast two-hybrid (Y2H) results for the Mi-EFF1/Minc17998 effector and the soybean GmHub4 (Glyma.06G076000), GmHub6 (Glyma.17G099100), GmHub10 (Glyma.19G008200), GmHub12 (Glyma.11G026400), GmHub17 (Glyma.02G105900), GmHub42 (Glyma.19G160900), GmHub47 (Glyma.09G174200), and GmHub61 (Glyma.02G178800) proteins (Table 1). Mi-EFF1/Minc17998 and the soybean GmHub proteins were expressed in yeast with a GAL4 activation domain (AD) and binding domain (BD) fusions. The interactions between these proteins were examined by monitoring histidine prototrophy. Yeast cells were transformed with a combination of DNA constructs, and proteins were expressed in yeast and assayed for interaction on selective synthetic medium (SD) in the presence of 5–10 mM 3-amino-1,2,4-triazol (3-AT) and cell dilutions at an optical density (OD_{600}) of 1.0, 0.1 or 0.01. **(B)** Dimerization and autoactivation assays with Mi-EFF1/Minc17998 and GmHub6 proteins. **(C)** Mi-EFF1/Minc17998 and GmHub6 protein interactions in Y2H screening. The protein-protein interactions were evaluated using GmHub6-AD + pGBK empty vector-BD and AtWWP1 (AT2G41020)-BD + NIG (AT4G13350)-AD as negative and positive controls, respectively. **(D)** *In planta* interaction between Mi-EFF1/Minc17998 and GmHub6 assessed by bimolecular fluorescence complementation (BiFC) assays. Fluorescence (YFP) images were acquired after the coexpression of the binary vectors pSITE BiFC cEFYP (GU734652) and nEYFP (GU734651) with the 35S:GmHub6-cYFP + 35S:Mi-EFF1/Minc17998 -nYFP fusion proteins in *N. tabacum* leaves. Negative controls were based on the empty vectors used in BiFC assays. Images are representative samples from three independent biological repeats. Scale bars are 20 μm.

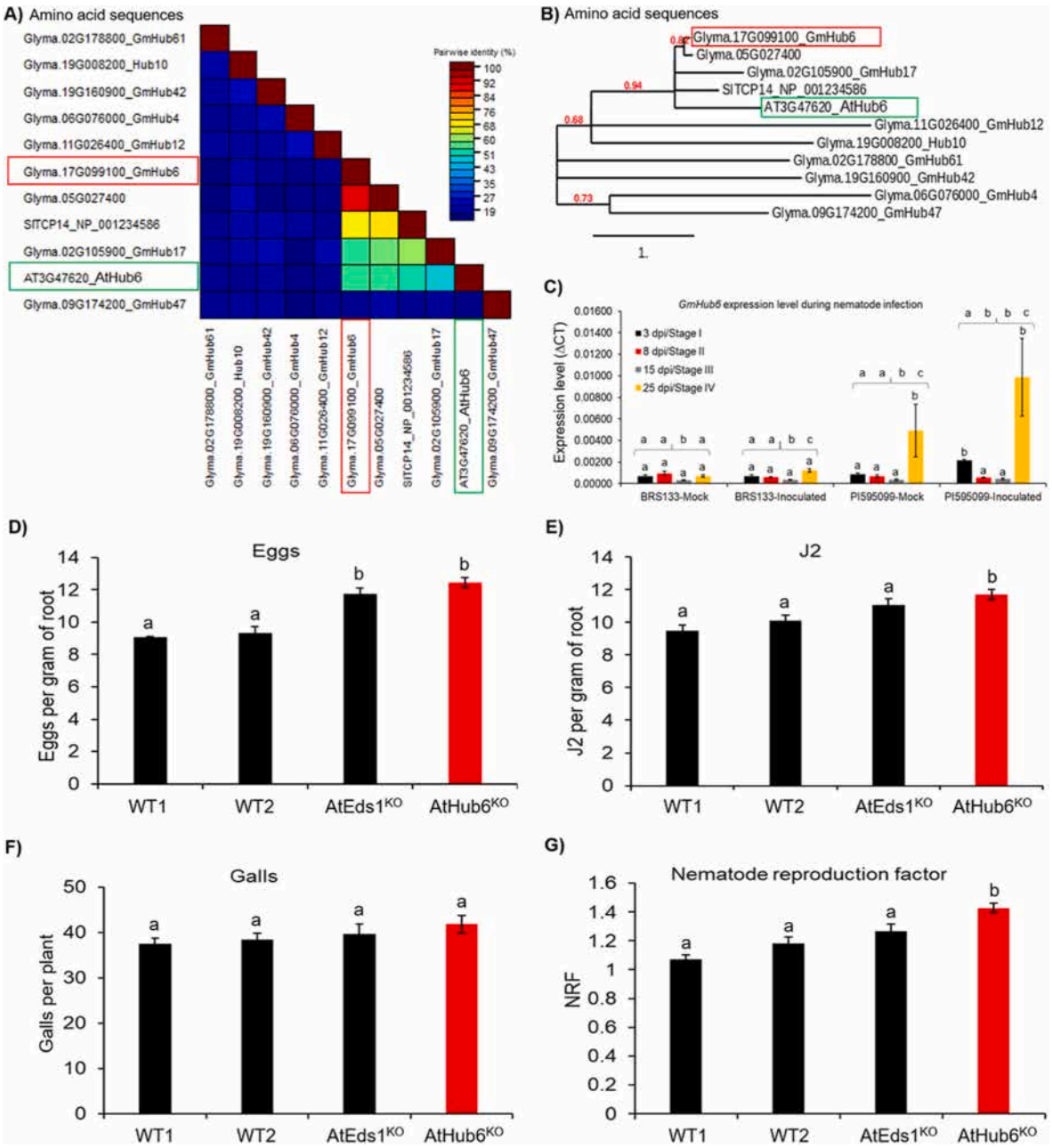

Fig. 3. *In silico* analysis and *GmHub6* (Glyma.17G099100) gene expression profile in soybean roots during *M. incognita* infection. **(A)** Pairwise sequence identity matrix from amino acid sequences generated using Sequence Demarcation Tool version 1.2 software. In addition, GmHub4 (Glyma.06G076000), GmHub6 (Glyma.17G099100), GmHub12 (Glyma.11G026400), GmHub17 (Glyma.02G105900), GmHub42 (Glyma.19G160900), GmHub47 (Glyma.09G174200), GmHub61 (Glyma.02G178800) (Table 1), one putative homologous protein of GmHub6 (Table 2), and *S. lycopersicum* SlTCP14 (NP_001234586) were included in this sequence analysis. **(B)** Evolutionary analysis of amino acid sequences generated by the Phylogeny.fr web service. Red and green boxes are highlight the GmHub6 and AtHub6 proteins, respectively, which were studied in this work. Soybean gene sequences were retrieved from *G. max Wm82.a2.v1* (BioProject: PRJNA19861) via the Phytozome v.12 database, while the *S. lycopersicum* SlTCP14 amino acid sequence (NP_001234586) was retrieved from the GenBank Database. **(C)** Expression profile of the *GmHub6* gene in the axillary roots of the conventional soybean cultivar BRS133 (susceptible) and genotype PI595099 (resistant), which are considered to present contrasting root-knot nematode resistance/susceptibility. The expression profile was measured in the mock-inoculated and *M. incognita* race 1-inoculated plants using RT-qPCR assays at 3, 8, 15, and 25 days postinoculation (dpi). The time points of 3, 8, 15, and 25 dpi correspond to development stages I (opening of the second trifoliate), II (opening of the fourth trifoliate), III (opening of the sixth trifoliate in cultivar BRS133 and beginning of flowering in genotype PI595099), and IV (beginning of flowering in cultivar BRS133 and the grain boot stage in genotype PI595099) in the plants maintained under greenhouse conditions. The expression level values were calculated using the $2^{-\Delta CT}$ method with the *GmCYP18* gene as an endogenous reference gene (Supplementary Table S1). Error bars represent confidence intervals corresponding to four biological replicates (each biological replicate was composed of four plants). Different letters in the graph bars indicate significant differences based on Tukey's test at the 5% level of significance. Susceptibility of the *A. thaliana AtHub6* (AT3G47620; *attcp14-5*; GK-611C04/CS458588) mutant (T-DNA insertion) line to *M. incognita* race 3 compared to the *A. thaliana* Col-0 ecotype (wild-type; WT) and the null mutant line for the *enhanced disease susceptibility 1* (AT3G48090; *Eds1*; SALK_034340) gene. **(D)** Number of eggs per gram of roots, **(E)** number of *M. incognita* J2 per gram of roots, **(F)** number of galls per plant, and **(G)** nematode reproduction factor (NRF) in *A. thaliana* WT (AtWT1 and AtWT2), *A. thaliana AtEds1* mutant ($AtEds1^{KO}$), and *A. thaliana AtHub6* mutant ($AtHub6^{KO}$). Error bars represent confidence intervals corresponding to three technical replicates (D, E, and G) or to each plant evaluated (F), while each treatment was composed of 15–20 plants. Different letters on the graph bars indicate significant differences based on Tukey's test at the 5% significance level. (For interpretation of the references to colour in this figure legend, the reader is referred to the Web version of this article.)

Table 2
Features of the soybean *GmHub6* (Glyma.17G099100) gene and its interactor genes retrieved from the *G. max* Wm82.a2.v1 (BioProject: PRJNA19861) genome dataset from the Phytozome v.12 database.

Gene ID	Gene function annotations	Gene length	Chromosome	Chromosome location (START)	Chromosome location (END)	CDD domain search	HMMER prediction	NLS motif
Glyma.17G099100	TCP family transcription factor	3003	Chr17	7811940	7814942	pfam03634	PF03634	yes
Glyma.01G014900	Inactive shikimate kinase like 2, alpha-crystallin domain (ACD)	4301	Chr01	1479986	1484286	cl00175 and cl31839	PF01202	no
Glyma.04G094000	Chaperone DNAJ-domain containing protein	1396	Chr04	8359193	8360588	pfam00226	PF00226	yes
Glyma.07G143100	Chaperone protein DNAJ-like protein	4672	Chr07	17046932	17051603	cl31697	no	no
Glyma.10G240200	Transcription factor TCP9	1075	Chr10	46871673	46872747	cl23822	PF03634	yes
Glyma.12G168300	TCP family transcription factor	2777	Chr12	32320419	32323195	pfam03634	PF03634	yes
Glyma.14G021600	Helicase-related//subfamily not named	2041	Chr14	1528273	1530313	COG0571 and cd00048	PF00035 and PF00636	no
Glyma.16G004300	TCP family transcription factor	1908	Chr16	237659	239566	pfam03634	PF03634	no
Glyma.18G296100	Small nuclear ribonucleoprotein 35 kDa protein	4256	Chr18	57314663	57318918	cd12237 and cl36939	PF00076	yes
Glyma.20G154400	Transcription factor TCP9	1833	Chr20	39340912	39342744	cl23822	PF03634	yes
Glyma.20G189400	Signal-recognition-particle GTPase	369	Chr20	42791357	42791725	cl28914	no	no

the resistant and susceptible soybean cultivars. In contrast, a higher expression level of the *GmHub6* gene was observed at 25 dpi in the resistant cultivar in both mock-treated and inoculated roots. Concerning *GmHub6* expression level in the four developmental stages (stage I, II, III, and IV) of the soybean plants, significant differences were observed from stage I to stage IV in both soybean cultivars. Thus, in both mock-inoculated and infected plants, the *GmHub6* gene expression level was finely modulated throughout plant development, which was more pronounced in the resistant soybean cultivar, mainly as a consequence of nematode infection.

3.5. *M. incognita* susceptibility assessment of the *A. thaliana AtHub6^{KO}*

The *A. thaliana AtHub6^{KO}* plants exhibited normal development, similar to WT plants (data not shown). To assess whether the interaction of the Mi-EFF1/Minc17998 effector with the soybean GmHub6 protein may be associated with an increase in plant susceptibility, the *AtHub6^{KO}* was inoculated with 250 *M. incognita* J2 individuals, and the evolution of parasitism was evaluated over time. The nematode penetration efficiency, post penetration development, and formation and morphology of the galls in *AtHub6^{KO}* plants were similar to those in the WT and *AtEds*1 control plants. However, at 40 dpi, the *AtHub6* plants showed a greater number of eggs and J2 individuals per gram of roots, a similar number of galls per plant, and a higher nematode reproduction factor (NRF) compared to the mock-inoculated mutant plants (Fig. 3D–G). These data indicate that plants in which the *AtHub6* gene was mutated were more susceptible to the nematode.

4. Discussion

Plants exhibit numerous mechanisms associated with defense against pathogens that are regulated in the presence or absence of pathogens to prioritize the development of the plant or the defense response [75–77]. The growth defense trade-off is essential to ensure plant survival and reproduction [78]. The development and defense pathways are closely related so that any disturbance in the cell cycle can trigger the plant immune system [79,80]. Initially, the root damage caused by RKN infection releases plant-derived compounds that act as damage-associated molecular patterns (DAMPs) and subsequently activate a PTI-like basal defense response [81]. Another step in PTI against RKNs may involve the recognition of PAMPs or nematode-associated molecular patterns (NAMPs), including ascarosides, cuticle, or chitin fragments [82].

In addition to inactivating host defenses, RKNs also need to modulate the host plant' cell cycle to successfully establish a feeding site [8,83,84]. The RKNs are sedentary endoparasitic pathogens that spend most of their life cycle inside roots and giant cells from the J2 entry to oviposition by adult females. This infective phase usually lasts about 20–35 days for *M. incognita,* and effector proteins are essential for nematode infection [85,86]. Since the first *M. incognita* genome sequence was reported [2,56], several effector proteins have been identified, and some have been characterized, but their role after their secretion into the host plant cell is still poorly understood [15,20,34,87].

In this study, we have contributed to the knowledge of the functional characteristics of the Mi-EFF1/Minc17998 effector and proposed a role of this effector in the parasitism of the host plant. Jaouannet et al. [37] and Quentin et al. [88] demonstrated that this effector is produced in the esophageal glands of parasitic juveniles, secreted in the feeding site and targeted to the nucleus, suggesting its involvement in the modulation of host cell metabolism. Herein, we showed that this effector exhibited low sequence identity and distant phylogenetic relationship with other well-known effectors, indicating a specific mode of action after delivery into the host plant. Furthermore, our data showed that the *Mi-EFF1/-Minc17998* gene is strongly upregulated during parasitism in the J2/J3, J3/J4, and female stages but is also expressed in eggs and preparasitic J2 individuals, suggesting the role of its product as a putative avirulence protein and its involvement in the formation of giant cells. A specific protein-protein interaction between Mi-EFF1/Minc17998 and the soybean GmHub6 protein was demonstrated, and the functional disruption of the GmHub6 protein has been speculated to occur in the context of plant parasitism. Considering that the GmHub6 protein could play an essential role similar to that of AtHub6/TCP14 in the regulation of the cell cycle, the plant growth and development [41–46] and the regulation of the plant's defense responses [38,42,47–49], this speculation is entirely plausible. Accordingly, several molecular interactions between nematode effectors and host plant proteins have already been characterized and associated with cell cycle modulation [8,83] and host defense suppression [25,30,87,89–91]. In our study, the data on the Mi-EFF1/Minc17998 effector and GmHub6 protein interaction, together with the increased susceptibility of the *AtHub6^{KO}* plants to *M. incognita* infection, suggest that this effector may be associated with cell cycle modulation and/or the suppression of plant defense responses. Similarly, Kim et al. [49], Li et al. [47] and Spears et al. [43] demonstrated that the *A. thaliana attcp8*, *attcp14*, and *attcp15* triple mutant exhibited impaired immune responses, while Yang et al. [48] showed that the AtTCP14 protein was targeted for degradation after interaction with the *P. syringae* HopBB1 effector.

Stam et al. [92] showed that the *Phytophthora capsici* CRN12_997 effector interacts with the tomato SlTCP14 (putative ortholog of the *GmHub6* and *AtHub6* genes) protein, reducing the SlTCP14 association

with nuclear chromatin and altering its subnuclear localization. Also, SlTCP14 overexpression enhances plant immunity to *P. capsici*, while the coexpression of the CRN12_997 effector abolishes this phenotype [92]. Thus, our data showed that the *GmHub6* gene was upregulated in response to *M. incognita* infection but only in the resistant soybean genotype, suggesting that its accumulation may be mainly associated with an improvement in the plant resistance. So, we believe that the Mi-EFF1/Minc17998 effector acts by interacting with the GmHub6 protein to primarily alter the cell cycle, which in turn activates the immune system. Subsequently, the functional disturbance of the GmHub6 protein in plant cells targeted by the nematode strongly impairs the host's defense responses and allows *M. incognita* to complete its life cycle.

Given this hypothesis, RNAi technology's use to target the Mi-EFF1/Minc17998 effector may be an interesting strategy to improving resistance to *M. incognita* in transgenic plants. This hypothesis is supported by the low genetic variability (approx. 0.02% of nucleotides) observed in protein-coding regions among different *M. incognita* races or isolates [93]. Besides, only slight variations in gene copy number and expression levels have been observed among different *M. incognita* isolates and races [94]. In contrast, the expression modulation of the *GmHub6* gene (or its orthologous genes in other crops of interest) via its overexpression or targeted transcriptional modulation using the CRISPR/dCas system [95] can be evaluated (or combined with an RNAi strategy) to improve plant resistance to RKNs.

In conclusion, several features of the *M. incognita* Mi-EFF1/Minc17998 effector and soybean GmHub proteins (especially the GmHub6 protein) have been highlighted, and we suggest their great importance for successful plant parasitism or plant resistance, respectively. The interaction between the Mi-EFF1/Minc17998 effector and the soybean GmHub6 protein is suggested to be a mechanism associated with a reduction in plant resistance to nematode infection via the disruption of GmHub6 activity. The high conservation of this effector in other *Meloidogyne* species suggests that NBTs based on RNAi could be developed to target and downregulate this effector gene in different RKN species or races. Therefore, our findings showed that the Mi-EFF1/Minc17998 effector and the soybean GmHub6 protein are powerful targets for the development of NBTs for nematode control in crops.

Authors' contributions

MFGS was the leading researcher for all the work and provided intellectual input and financial support. MFGS, RRF, and RAGM selected the soybean proteins and nematode effector and planned the experiments. JFA, RRF, and MGS performed soybean hub gene amplification, cloning, sequencing, and gene sequence analysis. RAGM, aided by RNL and BPM, performed the protein-protein interaction assays. MFB, RAGM, and VSM produced the *M. incognita* inoculum, performed plant inoculation, and evaluated all bioassays. MFB performed the *in silico* analysis and evaluated gene expression levels in nematodes and soybeans. RCT performed the data mining of 15 transcriptome libraries and the differential expression profiles of the nematode effectors. MFGS, MCMS, EVSA, MELS, DF, LLPM, TPR, and FV provided intellectual input. MFB wrote the manuscript. All authors read and approved the final version.

Ethics approval and consent to participate

Not applicable.

Consent for publication

Not applicable.

Declaration of competing interest

The authors declare that they have no known competing financial interests or personal relationships that could have appeared to influence the work reported in this paper.

Acknowledgments

We are grateful to EMBRAPA, UCB, CAPES, CNPq, INCT PlantStress Biotech, and FAP-DF for financial and scientific support. RAGM is grateful to CAPES for the doctoral research fellowship, while MFB is grateful to CNPq for the postdoctoral research fellowship (PDJ 150936/2018-4). We also thank Dr. Bum-Soo Hahn for providing access to the transcriptome datasets of different *M. incognita* life stages and Bruna Medeiros Pereira for kindly providing the initial inoculum of *M. incognita*.

Appendix A. Supplementary data

Supplementary data to this article can be found online at https://doi.org/10.1016/j.pmpp.2021.101630.

Supplemental Table 1
Primer sequences used in this study.

Gene ID	Gene name	Primer name	Primer sequence (5′- 3′)	*Tm* (°C)	GC%	Length (bp)
Minc3s01352g23040	*Mi-EFF1/Minc17998*	Minc17998q(F)	CAATCGTTAGGCGTGAATCGG	60	52	125
		Minc17998q(R)	GGATGGACGGCATTGCATTT	60	50	
Minc3s08501g42315	*Mi18S*	Mi18Sq(F)	CTGTGATGCCCTTAGATGTCC	60	52	170
		Mi18Sq(R)	TGATGACTCGCACTTACTTGG	60	52	
Glyma.17G099100	*GmHub6*	Glyma.17G099100q1(F)	CCCAAGCCGCAAAAGAAGAC	60	55	114
		Glyma.17G099100q1(R)	GGAATAGCGCCTGCACTAGA	59	55	
Glyma.12G024700	*GmCYP18*	GmCYP18(F)	CCCCTCCACTACAAAGGCTCG	60	61	154
		GmCYP18(R)	CGGGACCAGTGTGCTTCTTCA	60	57	

References

[1] D.L. Trudgill, V.C. Blok, Apomictic, polyphagous root-knot nematodes: exceptionally successful and damaging biotrophic root pathogens, Annu. Rev. Phytopathol. 39 (2001) 53–77.

[2] P. Abad, J. Gouzy, J.-M. Aury, P. Castagnone-Sereno, E.G.J. Danchin, E. Deleury, et al., Genome sequence of the metazoan plant-parasitic nematode *Meloidogyne incognita*, Nat. Biotechnol. 26 (2008) 909.

[3] P. Castagnone-Sereno, E.G.J. Danchin, L. Perfus-Barbeoch, P. Abad, Diversity and evolution of Root-knot nematodes, genus *Meloidogyne*: new insights from the genomic Era, Annu. Rev. Phytopathol. 51 (1) (2013) 203–220.

[4] A. Triantaphyllou, H. Hirschmann (Eds.), Post Infection Development of *Meloidogyne incognita* Chitwood 1949 (Nematoda-Heteroderidae), Annales de l'Institut Phytopathologique Benaki, 1960.

[5] G.C. Bernard, M. Egnin, C. Bonsi, The Impact of Plant-Parasitic Nematodes on Agriculture and Methods of Control, Nematology - Concepts, Diagnosis and Control, 2017.

[6] J. de Almeida Engler, P. Vieira, N. Rodiuc, M.F. Grossi de Sa, G. Engler, Chapter four - the plant cell cycle machinery: usurped and modulated by plant-parasitic nematodes, in: C. Escobar, C. Fenoll (Eds.), Advances in Botanical Research, vol. 73, Academic Press, 2015, pp. 91–118.

[7] N. Shukla, R. Yadav, P. Kaur, S. Rasmussen, S. Goel, M. Agarwal, et al., Transcriptome analysis of root-knot nematode (*Meloidogyne incognita*)-infected tomato (*Solanum lycopersicum*) roots reveals complex gene expression profiles and metabolic networks of both host and nematode during susceptible and resistance responses, Mol. Plant Pathol. 19 (3) (2018) 615–633.

[8] J.D. Antonino de Souza Junior, O. Pierre, R.R. Coelho, M.F. Grossi-de-Sa, G. Engler, J. de Almeida Engler, Application of nuclear volume measurements to comprehend the cell cycle in root-knot nematode-induced giant cells, Front. Plant Sci. 8 (2017) 961.

[9] J. de Almeida Engler, K. Van Poucke, M. Karimi, R. De Groodt, G. Gheysen, G. Engler, et al., Dynamic cytoskeleton rearrangements in giant cells and syncytia of nematode-infected roots, Plant J. 38 (1) (2004) 12–26.

[10] J. de Almeida Engler, T. Kyndt, P. Vieira, E. Van Cappelle, V. Boudolf, V. Sanchez, et al., CCS52 and DEL1 genes are key components of the endocycle in nematode-induced feeding sites, Plant J. 72 (2) (2012) 185–198.

[11] R.G. Carneiro, P. Mazzafera, L.C.C.B. Ferraz, T. Muraoka, P.C.O. Trivelin, Uptake and translocation of nitrogen, phosphorus and calcium in soybean infected with *Meloidogyne incognita* and *M. javanica*, Fitopatol. Bras. 27 (2002) 141–150.

[12] H. Melakeberhan, J.M. Webster, R.C. Brooke, J.M. D'Auria, M. Cackette, Effect of *Meloidogyne incognita* on plant nutrient concentration and its influence on the physiology of beans, J. Nematol. 19 (3) (1987) 324–330.

[13] P. Lu, R.F. Davis, R.C. Kemerait, M.W. van Iersel, H. Scherm, Physiological effects of *Meloidogyne incognita* infection on cotton genotypes with differing levels of resistance in the greenhouse, J. Nematol. 46 (4) (2014) 352–359.

[14] F.X. Gillet, C. Bournaud, J.D. Antonino de Souza Junior, M.F. Grossi-de-Sa, Plant-parasitic nematodes: towards understanding molecular players in stress responses, Ann. Bot. 119 (5) (2017) 775–789.

[15] B. Lin, K. Zhuo, P. Wu, R. Cui, L.-H. Zhang, J. Liao, A novel effector protein, Mj-NULG1a, targeted to giant cell nuclei plays a role in *Meloidogyne javanica* parasitism, Mol. Plant Microbe Interact. 26 (1) (2013) 55–66.

[16] M.T. Melillo, P. Leonetti, A. Leone, P. Veronico, T. Bleve-Zacheo, ROS and NO production in compatible and incompatible tomato-*Meloidogyne incognita* interactions, Eur. J. Plant Pathol. 130 (4) (2011) 489–502.

[17] P. Manosalva, M. Manohar, S.H. von Reuss, S. Chen, A. Koch, F. Kaplan, et al., Conserved nematode signalling molecules elicit plant defenses and pathogen resistance, Nat. Commun. 6 (2015) 7795.

[18] D. Holscher, S. Dhakshinamoorthy, T. Alexandrov, M. Becker, T. Bretschneider, A. Buerkert, et al., Phenalenone-type phytoalexins mediate resistance of banana plants (*Musa* spp.) to the burrowing nematode *Radopholus similis*, Proc. Natl. Acad. Sci. Unit. States Am. 111 (1) (2014) 105–110.

[19] L.-A. Kong, D.-Q. Wu, W.-K. Huang, H. Peng, G.-F. Wang, J.-K. Cui, et al., Large-scale identification of wheat genes resistant to cereal cyst nematode *Heterodera avenae* using comparative transcriptomic analysis, BMC Genom. 16 (1) (2015) 801.

[20] S. Bellafiore, Z. Shen, M.N. Rosso, P. Abad, P. Shih, S.P. Briggs, Direct identification of the *Meloidogyne incognita* secretome reveals proteins with host cell reprogramming potential, PLoS Pathog. 4 (10) (2008), e1000192.

[21] R. Shinya, H. Morisaka, T. Kikuchi, Y. Takeuchi, M. Ueda, K. Futai, Secretome analysis of the pine wood nematode *Bursaphelenchus xylophilus* reveals the tangled roots of parasitism and its potential for molecular mimicry, PloS One 8 (6) (2013), e67377.

[22] G. Dubreuil, E. Deleury, M. Magliano, M. Jaouannet, P. Abad, M.N. Rosso, Peroxiredoxins from the plant parasitic root-knot nematode, *Meloidogyne incognita*, are required for successful development within the host, Int. J. Parasitol. 41 (3–4) (2011) 385–396.

[23] M.F. Basso, I.T. Lourenço-Tessutti, R.A.G. Mendes, C.E.M. Pinto, C. Bournaud, F.-X. Gillet, et al., *MiDaf16-like* and *MiSkn1-like* gene families are reliable targets to develop biotechnological tools for the control and management of *Meloidogyne incognita*, Sci. Rep. 10 (1) (2020) 6991.

[24] J. Xie, S. Li, C. Mo, G. Wang, X. Xiao, Y. Xiao, A novel *Meloidogyne incognita* effector Misp12 suppresses plant defense response at latter stages of nematode parasitism, Front. Plant Sci. 964 (2016).

[25] B. Lin, K. Zhuo, S. Chen, L. Hu, L. Sun, X. Wang, et al., A novel nematode effector suppresses plant immunity by activating host reactive oxygen species-scavenging system, New Phytol. (3) (2016) 1159–1173.

[26] C. Bournaud, F.-X. Gillet, A.M. Murad, E. Bresso, E.V.S. Albuquerque, M.F. Grossi-de-Sa, *Meloidogyne incognita* PASSE-MURAILLE (MiPM) gene encodes a cell-penetrating protein that interacts with the CSN5 subunit of the COP9 signalosome, Front. Plant Sci. 9 (904) (2018).

[27] C.N. Nguyen, L. Perfus-Barbeoch, M. Quentin, J. Zhao, M. Magliano, N. Marteu, et al., A root-knot nematode small glycine and cysteine-rich secreted effector, MiSGCR1, is involved in plant parasitism, New Phytol. 217 (2) (2018) 687–699.

[28] M. Grossi-de-Sa, A.-S. Petitot, D.A. Xavier, M.E.L. Sá, I. Mezzalira, M.A. Beneventi, et al., Rice susceptibility to root-knot nematodes is enhanced by the *Meloidogyne incognita* MSP18 effector gene, Planta 250 (4) (2019) 1215–1227.

[29] Q. Shi, Z. Mao, X. Zhang, J. Ling, R. Lin, X. Zhang, et al., The novel secreted *Meloidogyne incognita* effector MiISE6 targets the host nucleus and facilitates parasitism in Arabidopsis, Front. Plant Sci. 9 (2018) 252.

[30] J. Zhao, L. Li, Q. Liu, P. Liu, S. Li, D. Yang, et al., A MIF-like effector suppresses plant immunity and facilitates nematode parasitism by interacting with plant annexins, J. Exp. Bot. 70 (20) (2019) 5943–5958.

[31] J. Niu, P. Liu, Q. Liu, C. Chen, Q. Guo, J. Yin, et al., Msp40 effector of root-knot nematode manipulates plant immunity to facilitate parasitism, Sci. Rep. 6 (1) (2016) 19443.

[32] B. Xue, N. Hamamouch, C. Li, G. Huang, R.S. Hussey, T.J. Baum, et al., The 8D05 parasitism gene of *Meloidogyne incognita* is required for successful infection of host roots, Phytopathology 103 (2) (2013) 175–181.

[33] N. Leelarasamee, L. Zhang, C. Gleason, The root-knot nematode effector MiPFN3 disrupts plant actin filaments and promotes parasitism, PLoS Pathog. 14 (3) (2018), e1006947.

[34] W.B. Rutter, T. Hewezi, S. Abubucker, T.R. Maier, G. Huang, M. Mitreva, et al., Mining novel effector proteins from the esophageal gland cells of *Meloidogyne incognita*, Mol. Plant Microbe Interact. 27 (9) (2014) 965–974.

[35] M.A. Ali, F. Azeem, H. Li, H. Bohlmann, Smart parasitic nematodes use multifaceted strategies to parasitize plants, Front. Plant Sci. 8 (1699) (2017).

[36] G. Huang, B. Gao, T. Maier, R. Allen, E.L. Davis, T.J. Baum, et al., A profile of putative parasitism genes expressed in the esophageal gland cells of the root-knot nematode *Meloidogyne incognita*, Mol. Plant Microbe Interact. 16 (5) (2003) 376–381.

[37] M. Jaouannet, L. Perfus-Barbeoch, E. Deleury, M. Magliano, G. Engler, P. Vieira, et al., A root-knot nematode-secreted protein is injected into giant cells and targeted to the nuclei, New Phytol. 194 (4) (2012) 924–931.

[38] M.S. Mukhtar, A.R. Carvunis, M. Dreze, P. Epple, J. Steinbrenner, J. Moore, et al., Independently evolved virulence effectors converge onto hubs in a plant immune system network, Science 333 (6042) (2011) 596–601.

[39] R. Wessling, P. Epple, S. Altmann, Y. He, L. Yang, S.R. Henz, et al., Convergent targeting of a common host protein-network by pathogen effectors from three kingdoms of life, Cell Host Microbe 16 (3) (2014) 364–375.

[40] A.I.M. Consortium, Evidence for network evolution in an Arabidopsis interactome map, Science 333 (6042) (2011) 601–607.

[41] K. Tatematsu, K. Nakabayashi, Y. Kamiya, E. Nambara, Transcription factor AtTCP14 regulates embryonic growth potential during seed germination in *Arabidopsis thaliana*, Plant J. 53 (1) (2008) 42–52.

[42] S. Li, The *Arabidopsis thaliana* TCP transcription factors: a broadening horizon beyond development, Plant Signal. Behav. 10 (7) (2015) e1044192-e.

[43] B.J. Spears, T.C. Howton, F. Gao, C.M. Garner, M.S. Mukhtar, W. Gassmann, Direct regulation of the EFR-dependent immune response by Arabidopsis TCP transcription factors, Mol. Plant Microbe Interact. 32 (5) (2019) 540–549.

[44] M. Kieffer, V. Master, R. Waites, B. Davies, TCP14 and TCP15 affect internode length and leaf shape in Arabidopsis, Plant J. 68 (1) (2011) 147–158.

[45] F. Resentini, A. Felipo-Benavent, L. Colombo, A. Blázquez Miguel, D. Alabadí, S. Masiero, TCP14 and TCP15 mediate the promotion of seed germination by gibberellins in *Arabidopsis thaliana*, Mol. Plant 8 (3) (2015) 482–485.

[46] Y. Peng, L. Chen, Y. Lu, Y. Wu, J. Dumenil, Z. Zhu, et al., The ubiquitin receptors DA1, DAR1, and DAR2 redundantly regulate endoreduplication by modulating the stability of TCP14/15 in Arabidopsis, Plant Cell 27 (3) (2015) 649–662.

[47] M. Li, H. Chen, J. Chen, M. Chang, I.A. Palmer, W. Gassmann, et al., TCP transcription factors interact with NPR1 and contribute redundantly to systemic acquired resistance, Front. Plant Sci. 9 (1153) (2018).

[48] L. Yang, P.J.P.L. Teixeira, S. Biswas, O.M. Finkel, Y. He, I. Salas-Gonzalez, et al., *Pseudomonas syringae* type III effector HopBB1 promotes host transcriptional repressor degradation to regulate phytohormone responses and virulence, Cell Host Microbe 21 (2) (2017) 156–168.

[49] S.H. Kim, G.H. Son, S. Bhattacharjee, H.J. Kim, J.C. Nam, P.D.T. Nguyen, et al., The Arabidopsis immune adaptor SRFR1 interacts with TCP transcription factors that redundantly contribute to effector-triggered immunity, Plant J. 78 (6) (2014) 978–989.

[50] G.L. Hartman, E.D. West, T.K. Herman, Crops that feed the World 2. Soybean-worldwide production, use, and constraints caused by pathogens and pests, Food Secur. 3 (1) (2011) 5–17.

[51] USDA, World Agricultural Production, United State Departament of Agriculture - Cirucular series WAP 2-2020, 2020.

[52] O.T. Hamawaki, R.L. Hamawaki, A.P.O. Nogueira, J.S. Glasenapp, C.D. L. Hamawaki, COd Silva, Evaluation of soybean breeding lineages to new sources of root-knot nematode resistance, Cienc. E Agrotecnol 43 (2019).

[53] V.C.G. Mazzetti, G.L. Visintin, I.P. Valério, J.N. Camera, C.C. Deuner, P.L. M. Soares, Reaction of soybean cultivars to *Meloidogyne javanica* and *Meloidogyne incognita*, Rev. Ceres 66 (2019) 220–225.

[54] M.F. Basso, P.C.G. Ferreira, A.K. Kobayashi, F.G. Harmon, A.L. Nepomuceno, H.B. C. Molinari, et al., MicroRNAs and new biotechnological tools for its modulation

and improving stress tolerance in plants, Plant Biotechnol. J. 17 (8) (2019) 1482–1500.
[55] M. Basso, F.B.M. Arraes, M. Grossi-de-Sa, V.J.V. Moreira, M. Alves-Ferreira, MF G-d-S, Insights into genetic and molecular elements for transgenic crop development, Front. Plant Sci. 11 (2020) 509.
[56] R. Blanc-Mathieu, L. Perfus-Barbeoch, J.-M. Aury, M. Da Rocha, J. Gouzy, E. Sallet, et al., Hybridization and polyploidy enable genomic plasticity without sex in the most devastating plant-parasitic nematodes, PLoS Genet. 13 (6) (2017), e1006777.
[57] R.Y.N. Lee, K.L. Howe, T.W. Harris, V. Arnaboldi, S. Cain, J. Chan, et al., WormBase 2017: molting into a new stage, Nucleic Acids Res. 46 (D1) (2017) D869–D874.
[58] B.M. Muhire, A. Varsani, D.P. Martin, SDT: a virus classification tool based on pairwise sequence alignment and identity calculation, PloS One 9 (9) (2014), e108277 e.
[59] A. Dereeper, V. Guignon, G. Blanc, S. Audic, S. Buffet, F. Chevenet, et al., Phylogeny.fr: robust phylogenetic analysis for the non-specialist, Nucleic Acids Res. 36 (2008) (Web Server issue):W465-9.
[60] R.C. Edgar, MUSCLE: multiple sequence alignment with high accuracy and high throughput, Nucleic Acids Res. 32 (5) (2004) 1792–1797.
[61] I. Choi, P. Subramanian, D. Shim, B.-J. Oh, B.-S. Hahn, RNA-Seq of plant-parasitic nematode *Meloidogyne incognita* at various stages of its development, Front. Genet. 8 (2017) 190.
[62] A. Szitenberg, L. Salazar-Jaramillo, V.C. Blok, D.R. Laetsch, S. Joseph, V. M. Williamson, et al., Comparative genomics of apomictic root-knot nematodes: hybridization, ploidy, and dynamic genome change, Genome Biol. Evol. 9 (10) (2017) 2844–2861.
[63] J. Schmutz, S.B. Cannon, J. Schlueter, J. Ma, T. Mitros, W. Nelson, et al., Genome sequence of the palaeopolyploid soybean, Nature 463 (7278) (2010) 178–183.
[64] D.M. Goodstein, S. Shu, R. Howson, R. Neupane, R.D. Hayes, J. Fazo, et al., Phytozome: a comparative platform for green plant genomics, Nucleic Acids Res. 40 (Database issue) (2012) D1178–D1186.
[65] A. Marchler-Bauer, M.K. Derbyshire, N.R. Gonzales, S. Lu, F. Chitsaz, L.Y. Geer, et al., CDD: NCBI's conserved domain database, Nucleic Acids Res. 43 (Database issue) (2015) D222–D226.
[66] T.J. Wheeler, S.R. Eddy, NHMMER: DNA homology search with profile HMMs, Bioinformatics 29 (19) (2013) 2487–2489.
[67] Ba AN. Nguyen, A. Pogoutse, N. Provart, A.M. Moses, NLStradamus: a simple Hidden Markov Model for nuclear localization signal prediction, BMC Bioinf. 10 (2009) 202.
[68] D. Szklarczyk, A.L. Gable, D. Lyon, A. Junge, S. Wyder, J. Huerta-Cepas, et al., STRING v11: protein-protein association networks with increased coverage, supporting functional discovery in genome-wide experimental datasets, Nucleic Acids Res. 47 (D1) (2019) D607–D613.
[69] G. Dubreuil, M. Magliano, M.P. Dubrana, J. Lozano, P. Lecomte, B. Favery, et al., *Tobacco rattle virus* mediates gene silencing in a plant-parasitic root-knot nematode, J. Exp. Bot. 60 (14) (2009) 4041–4050.
[70] T.D. Schmittgen, K.J. Livak, Analyzing real-time PCR data by the comparative CT method, Nat. Protoc. 3 (2008) 1101.
[71] I.P. Calil, I.P.S. Quadros, T.C. Araújo, C.E.M. Duarte, B.C. Gouveia-Mageste, J.C. F. Silva, et al., A WW domain-containing protein forms immune nuclear bodies against begomoviruses, Mol. Plant 11 (12) (2018) 1449–1465.
[72] R.S. Hussey, K.R. Barker, A comparison of methods of collecting inocula of *Meloidogyne* spp., including a new technique, Plant Dis. Rep. 57 (1973) 1025–1028.
[73] M.A. Beneventi, O.B. da Silva Jr., M.E.L. de Sá, A.A.P. Firmino, R.M.S. de Amorim, E.V.S. Albuquerque, et al., Transcription profile of soybean-root-knot nematode interaction reveals a key role of phythormones in the resistance reaction, BMC Genom. 14 (2013) 322.
[74] D.W. Bybd, T. Kirkpatrick, K.R. Barker, An improved technique for clearing and staining plant tissues for detection of nematodes, J. Nematol. 15 (1) (1983) 142–143.
[75] Z. Bao, H. Yang, J. Hua, Perturbation of cell cycle regulation triggers plant immune response via activation of disease resistance genes, Proc. Natl. Acad. Sci. Unit. States Am. 110 (6) (2013) 2407–2412.
[76] M. Fan, M.Y. Bai, J.G. Kim, T. Wang, E. Oh, L. Chen, et al., The bHLH transcription factor HBI1 mediates the trade-off between growth and pathogen-associated molecular pattern-triggered immunity in Arabidopsis, Plant Cell 26 (2) (2014) 828–841.
[77] N.B. Eloy, M. de Freitas Lima, P.C.G. Ferreira, D. Inzé, The role of the anaphase-promoting complex/cyclosome in plant growth, Crit. Rev. Plant Sci. 34 (5) (2015) 487–505.
[78] J. Neuser, C.C. Metzen, B.H. Dreyer, C. Feulner, J.T. van Dongen, R.R. Schmidt, et al., HBI1 mediates the trade-off between growth and immunity through its impact on apoplastic ROS homeostasis, Cell Rep. 28 (7) (2019) 1670–1678, e3.
[79] Z. Bao, J. Hua, Linking the cell cycle with innate immunity in Arabidopsis, Mol. Plant 8 (7) (2015) 980–982.
[80] R. Eichmann, P. Schäfer, Growth versus immunity - a redirection of the cell cycle? Curr. Opin. Plant Biol. 26 (2015) 106–112.
[81] S. Hou, Z. Liu, H. Shen, D. Wu, Damage-associated molecular pattern-triggered immunity in plants, Front. Plant Sci. 10 (646) (2019) 1–16.
[82] J. Holbein, F.M.W. Grundler, S. Siddique, Plant basal resistance to nematodes: an update, J. Exp. Bot. 67 (7) (2016) 2049–2061.
[83] J. de Almeida Engler, G. Gheysen, Nematode-induced endoreduplication in plant host cells: why and how? Mol. Plant Microbe Interact. 26 (1) (2013) 17–24.
[84] R.R. Coelho, P. Vieira, J.D. Antonino de Souza Júnior, C. Martin-Jimenez, L. De Veylder, J. Cazareth, et al., Exploiting cell cycle inhibitor genes of the KRP family to control root-knot nematode induced feeding sites in plants, Plant Cell Environ. 40 (7) (2017) 1174–1188.
[85] D.E. Cook, C.H. Mesarich, B.P.H.J. Thomma, Understanding plant immunity as a surveillance system to detect invasion, Annu. Rev. Phytopathol. 53 (1) (2015) 541–563.
[86] M.S. Silva, F.B.M. Arraes, M.A. Campos, M. Grossi-de-Sa, D. Fernandez, E. S. Cândido, et al., Review: potential biotechnological assets related to plant immunity modulation applicable in engineering disease-resistant crops, Plant Sci. 270 (2018) 72–84.
[87] J. Mejias, N.M. Truong, P. Abad, B. Favery, M. Quentin, Plant proteins and processes targeted by parasitic nematode effectors, Front. Plant Sci. 10 (970) (2019).
[88] M. Quentin, P. Abad, B. Favery, Plant-parasitic nematode effectors target host defense and nuclear functions to establish feeding cells, Front. Plant Sci. 4 (53) (2013).
[89] A. Goverse, G. Smant, The activation and suppression of plant innate immunity by parasitic nematodes, Annu. Rev. Phytopathol. 52 (1) (2014) 243–265.
[90] N. Hamamouch, C. Li, T. Hewezi, T.J. Baum, M.G. Mitchum, R.S. Hussey, et al., The interaction of the novel 30C02 cyst nematode effector protein with a plant beta-1,3-endoglucanase may suppress host defense to promote parasitism, J. Exp. Bot. 63 (10) (2012) 3683–3695.
[91] L.J. Davies, L. Zhang, A.A. Elling, The *Arabidopsis thaliana* papain-like cysteine protease RD21 interacts with a root-knot nematode effector protein, Nematology 17 (6) (2015) 655–666.
[92] R. Stam, G.B. Motion, P.C. Boevink, E. Huitema, A Conserved Oomycete CRN Effector Targets and Modulates Tomato TCP14-2 to Enhance Virulence, 2013. BioRxiv 001248.
[93] G.D. Koutsovoulos, E. Marques, M.-J. Arguel, L. Duret, A.C.Z. Machado, R.M.D. G. Carneiro, et al., Population genomics supports clonal reproduction and multiple independent gains and losses of parasitic abilities in the most devastating nematode pest, Evol. Appl. 13 (2) (2019) 442–457.
[94] P. Castagnone-Sereno, K. Mulet, E.G.J. Danchin, G.D. Koutsovoulos, M. Karaulic, M. Da Rocha, et al., Gene copy number variations as signatures of adaptive evolution in the parthenogenetic, plant-parasitic nematode *Meloidogyne incognita*, Mol. Ecol. 28 (10) (2019) 2559–2572.
[95] J.F. Roca Paixão, F.-X. Gillet, T.P. Ribeiro, C. Bournaud, I.T. Lourenço-Tessutti, D. D. Noriega, et al., Improved drought stress tolerance in Arabidopsis by CRISPR/dCas9 fusion with a Histone AcetylTransferase, Sci. Rep. 9 (1) (2019) 8080.